Preventing co-infection: a viral strategy with short-term benefits and long-term drawbacks

Michael Hunter[1] **and Diana Fusco**[1,*]

[1]Cavendish Laboratory, University of Cambridge, Cambridge, CB3 0HE, United Kingdom
[*]df390@cam.ac.uk

ABSTRACT

Viral co-infection occurs when multiple distinct viral particles infect the same host. This can impact viral evolution through intracellular interactions, complementation, reassortment and recombination. In nature many viral species are found to have a wide range of mechanisms to prevent co-infection, which raises the question of how viral evolution is impacted by this strategic choice. Here, we address this question in a model viral system, the ubiquitous bacteriophage and its host bacteria. Using a stochastic model of phage-host interactions in agent-based simulations, we first characterise the behaviour of neutral mutants and find that co-infection decreases the strength of genetic drift. We then quantify how variations in the phage life history parameters affect viral fitness. Importantly, we find that the growth rate (dis)advantage associated with variations in life history parameters can be dramatically different from the competitive (dis)advantage measured in direct-competition simulations. Additionally, we find that co-infection facilitates the fixation of beneficial mutations and the removal of deleterious ones, suggesting that selection is more efficient in co-infecting populations. We also observe, however, that in populations which allow co-infection, a mutant that prevents it displays a substantial competitive advantage over the rest of the population, and will eventually fix even if it displays a much lower growth rate in isolation. Our findings suggest that while preventing co-infection can have a negative impact on the long-term evolution of a viral population, in the short-term it is ultimately a winning strategy, possibly explaining the prevalence of phage capable of preventing co-infection in nature.

Introduction

Bacteriophages (phages) are viruses that infect and replicate within bacteria. Much like many other viruses, reproduction in lytic phage is typically characterised by several key steps: adsorption to a host cell, injection of viral genetic material, hijacking of host machinery, intracellular production of new phage, and finally, the release of progeny upon cell lysis. Phages represent one of the most ubiquitous and diverse organisms on the planet, and competition for viable host can lead to different strains or even species of phage co-infecting the same bacterial cell, ultimately resulting in the production of more than one type of phage (Fig. 1a)[1,2]. Interestingly, several phages have mechanisms that prevent co-infection. This can be achieved by preventing further adsorption of phage, or by preventing the successful injection of subsequent phage DNA[3,4]. For instance, bacteriophage T5 encodes a lipoprotein (Llp) that is synthesised by the host at the start of infection, preventing superinfection by blocking the outer membrane receptor site (FhuA protein)[5,6]. Furthermore, bacteriophage T4 encodes two proteins, Imm and Sp, that prevent superinfection by other T-even phages by inhibiting the degradation of bacterial peptidoglycan and preventing the transfer of DNA across the membrane respectively[7,8]. Given that populations which allow and prevent co-infection both exist in nature, it is natural to wonder what impact either strategy has on the evolution of viral populations.

The evolutionary impact of co-infection in viral populations has been studied in various contexts with regards to intracellular interactions and competition[9–16]. Co-infection allows for the exchange of genetic material between viruses through recombination, which can increase diversity and improve the efficiency of selection, but may also decrease fitness by promoting the presence of deleterious mutants at low frequencies[17–19]. Additionally, in RNA viruses with segmented genomes, co-infection can lead to hybrid offspring containing re-assorted mixtures of the parental segments (reassortment). This mechanism can in principle improve the selection efficiency, as re-assorted segments may generate highly deleterious variants that can be easily purged from the population[20]. Co-infection can also lead to viral complementation however, where defective viruses can benefit from superior products generated by ordinary viruses inside the host[20–24]. This process increases the diversity of the population, but ultimately weakens selection by allowing deleterious individuals to persist in the population for longer[20,21].

For co-infection to occur, viruses must exist in an environment where they outnumber available host, so that the number of virus per host (infection multiplicity) is greater than one. The impact of infection multiplicity has been studied in a variety of experimental settings[22,23,25–29]. For instance, high multiplicity of infection in RNA phage $\phi 6$ has been shown to result in a behaviour conforming to the Prisoner's Dilemma strategy in game theory, and a reduction in viral diversity[25–28,30]. The impact of infection multiplicity on viral dynamics has also been studied mathematically in a variety of contexts[31], in particular in the

context of human immunodeficiency virus (HIV) infections[17,18,32–37], and in terms of the consequences for the diversity and evolution of the viral population[17,18,34,38–43].

While there is a wealth of research examining the complex interplay between the various intracellular interactions and their impact on the viral dynamics, there is a relative lack of understanding surrounding how the fundamental co-infection dynamic (absent of any intracellular interactions) affects the evolution of the viral population, particularly when it comes to basic evolutionary outcomes such as mutant fixation probabilities. It has been shown that absent of intracellular interactions, high multiplicity of infection can promote the presence of disadvantageous mutants in the short term, but make them less likely in the long term[44,45]. However, while increasing the infection multiplicity in co-infecting populations does increase the *likelihood* of co-infection, it is not the same as comparing populations that either allow or forbid co-infection completely, therefore making it difficult to draw conclusions about the dis(advantages) of either strategy. Additionally, how the evolutionary outcomes in each case depend on the parameters describing the viral life-cycle (adsorption rate, incubation period and burst size) has not been addressed.

Here, we investigate how allowing or preventing co-infection impacts the evolutionary fate of neutral and non-neutral variants in a simulated well-mixed phage population with constant, but limited, availability of host. We first quantify the effective population size of co-infecting and non co-infecting populations to estimate how these strategies affect genetic drift - the stochastic change in frequency of neutral alleles in the population. We then turn our attention to the effect of non-neutral mutations on the phage growth rate in isolation, alongside their impact on competitive ability. Having characterised both the neutral dynamics and the fitness of different variants, we put both aspects together to explore the balance between drift and selection in co-infecting and non co-infecting populations. This is achieved by measuring the probability of fixation of single, non-neutral mutants. As a final comparison of the two strategies, we consider the outcome of a mutation which changes whether an individual is capable of preventing co-infection or not.

Methods

Computational modelling framework

We study the evolutionary dynamics of phage infection using a stochastic agent-based model. We simulate a well-mixed population of phages (V) interacting with a population of host bacteria that is kept at a constant density, as would be achieved by a turbidostat[46,47]. Each phage has a defining set of life history parameters, namely an adsorption rate α, an incubation period τ and a burst size β, and each bacteria can either be in an uninfected B or an infected I state.

During each timestep, adsorption, phage replication within the host and lysis occur. The number of infecting phage V_I in each step is drawn from a Poisson distribution whose mean corresponds to the expectation value $\alpha V(B+I)$. The infecting phage are removed from the pool of free phage, and V_I bacteria are chosen with a uniform probability to be the infection target. Already infected bacteria can be chosen for repeated infection, and multiple phage can infect the same host in a single timestep. In both co-infecting and non co-infecting scenarios, the final burst size β and lysis time τ of the host are set by the first phage to infect it. This choice was made for the sake of simplicity, given the complex and varied nature of co-infection mechanisms[1,2]. In the case where multiple phage infect the same host in a single timestep, the 'first' phage is chosen randomly among those infecting the host.

In the case where no co-infection can occur, following a given number of steps τ after initial infection, the bacteria will lyse, releasing new phage into the pool of free phage. The number of phage released Y is drawn from a Poisson distribution with mean β.

In the case where co-infection can occur, pseudo-populations tracking the growth of phage inside the host are used (see Fig. 1b). During the intermediate steps between initial infection and lysis, the total number of phage inside the host increases at a constant rate β/τ, determined by the initial infecting phage. In this work we will focus on the case where there are only two distinct types of phage in the population. Consequently, following co-infection the new phage that grow in each step are divided according to the proportion of each type currently inside the host at that time, resulting in two pseudo-populations p_a and p_b. These choices were made based on previous observations that there is a positive linear relationship between lysis time and burst size[48], and to reflect the intracellular competition for the host's resources. At the point of lysis, the total number of phage released Y is again drawn from a Poisson distribution with mean β. The number of phage released of one type Y_a is then drawn from a binomial distribution with Y attempts and probability $p_a/(p_a+p_b)$ of success, with any remaining phage being the other type ($Y_b = Y - Y_a$).

Following lysis, the lysed bacteria are immediately replaced with a new, un-infected host, resulting in a bacterial population of constant size. We also introduce a decay, or removal, of free phage at rate δ, which accounts for natural phage decay and the outflow of the turbidostat system.

Simulations were initialised with B_0 uninfected bacteria and $2B_0$ "resident" phage, and then run until the phage, uninfected bacteria and infected bacteria populations each reached a steady state value (V_{ss}, B_{ss} and I_{ss} respectively), determined by a

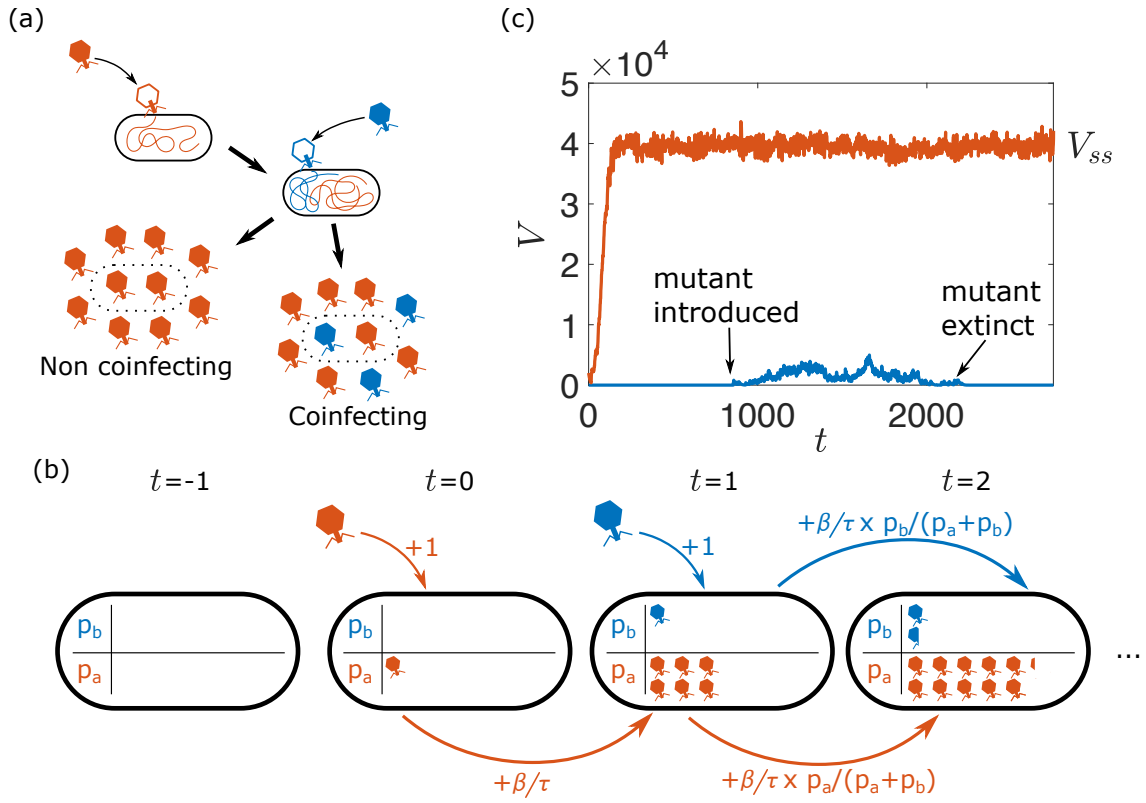

Figure 1. (a): In non co-infecting scenarios, all of the progeny released as the cell lyses are copies of the initial infecting phage, whereas when co-infecting in permitted, the progeny are split between both types of phage. (b): During co-infection, sudo-populations p_a and p_b are used to represent the growth of phage inside the host cells. These populations increase by 1 whenever a phage infects the host, and the total number of phage $(p_a + p_b)$ increases by β/τ in each time-step, with each population's increase being proportional to their relative size in the previous step. (c): An example realisation of the simulation. The resident phage population initially grows until it reaches a steady state, at which point a mutant phage is introduced to the population, and the simulation is run until extinction or fixation of the mutant.

constant running average of V (Fig. 1c). This steady state arises due to a balance between phage production and loss and it is independent on the initial number of phages (Supporting Information, Fig. S1).

Measuring effective population size of the phage population

It is expected that the heterozygosity H will decay due to genetic drift in our simulations, and consistent with previous work[49], we find that the decay is exponential at long times: $H \propto e^{-\Lambda t}$ (Supporting Information). This allows us to express the decay rate, in units of generations, in terms of an effective population size $\Lambda \equiv 2/N_e$ (Moran model[50]).

We track the viral heterozygosity H as a function of time, which in our biallelic viral population is given by

$$H = 2\langle f(1-f)\rangle \tag{1}$$

where f and $(1-f)$ represent the frequencies of two neutral labels in the population, and $\langle . \rangle$ indicates the average over independent simulations. $H(t)$ can be understood to be the time-dependent probability that two individuals chosen from the population have different labels.

To determine the generation time T, we first calculate the *net reproduction rate* R_0, which essentially represents the number of offspring an individual would be expected to produce if it passed through its lifetime conforming to the age-specific fertility and mortality rates of the population at a given time (i.e. taking into account the fact that some individuals die before reproducing). R_0 can be calculated as

$$R_0 = \sum l_t m_t, \tag{2}$$

where l_t represents the proportion of individuals surviving to age t, and m_t represents the average number of offspring produced at age t.

First, the term l_t is the proportion of phages surviving to age t. There are two mechanisms in our simulations by which phages can 'die:' either by decaying with rate δ, or by adsorbing to an infected host with rate αI_{ss}. In a sufficiently small timestep Δt, these rates correspond to probabilities $\delta\Delta t$ and $\alpha I_{ss}\Delta_t$, respectively. This means that the probability of a phage surviving to age t will be given by $l_t = (1-\delta\Delta t - \alpha I_{ss}\Delta t)^{t/\Delta t}$.

Now if we consider the average number of offspring m_t produced at age t, we can initially say that for all ages prior to the lysis time $m_t = 0$. After the lysis time, the average number of offspring produced will be given by the probability of successfully infecting a viable host in the timestep $(\alpha B_{ss}\Delta t)$, multiplied by the yield of new phage $(\beta - 1)$. This information is presented in Table 1 for illustrative purposes.

Table 1. R_0 **calculation.**

t	l_t	m_t
0	1	0
1	(1-δ-αI_{ss})	0
2	(1-δ-αI_{ss})^2	0
3	(1-δ-αI_{ss})^3	0
...	...	...
τ	(1-δ-αI_{ss})$^\tau$	$\alpha B_{ss}(\beta-1)$
$\tau+1$	(1-δ-αI_{ss})$^{\tau+1}$	$\alpha B_{ss}(\beta-1)$
...	...	...

In the limit where $\Delta t \to 0$, this will result in a net reproductive rate of the form

$$R_0 = \lim_{\Delta t\to 0}\sum_{t=0}^{\infty} m_t l_t = \lim_{\Delta t\to 0}\sum_{t=0}^{\infty} \Delta t\,\alpha B_{ss}(\beta-1)(1-\Delta t(\delta+\alpha I_{ss}))^{t/\Delta t}, \tag{3}$$

$$= \int_{t=\tau}^{\infty} \alpha B_{ss}(\beta-1)e^{-(\delta+\alpha I_{ss})t}\,\mathrm{d}t, \tag{4}$$

where the integral starts at τ because no offspring are produced prior to that point, and we have used the approximation that $e^x \approx 1+x$ for small x.

To then calculate the generation time T, defined here as the average interval between the birth of an individual and the birth of its offspring, we use the formula

$$T = \lim_{\Delta t\to 0}\frac{\sum t l_t m_t}{R_0}, \tag{5}$$

$$= \frac{\int_{t=\tau}^{\infty} t\,\alpha B_{ss}(\beta-1)e^{-(\delta+\alpha I_{ss})t}\,\mathrm{d}t}{R_0}. \tag{6}$$

For the parameters used as the typical resident parameters in the main text ($\alpha = 3\times10^{-6}$, $\tau = 15$, $\delta = 0.1$ and $B_0 = 1000$) this yields a generation time of T=24.8136 min.

Measuring mutant fitness and growth rate

We start by defining a selective advantage s_{growth} in terms of the exponential growth rate r of the population in isolation[51]:

$$s_{growth} = \frac{r_{mut}}{r_{res}} - 1. \tag{7}$$

where s_{growth} here represents the selective (dis)advantage of the mutant population (*mut*) over the resident population (*res*). We determine the exponential growth rate by performing a linear fit to the log-transformed population as a function of time, and then take the mean rate from 500 independent simulations. It should be noted that as there is only one type of phage in these simulations, the growth rate of both co-infecting and non co-infecting populations is the same.

We also characterised the fitness of mutants in a competitive setting. This was achieved by simulating a resident population until a steady state was reached, and then replacing 50% of the population with the mutant. In this competitive environment, mutants may experience a different selective advantage s_{comp} to that experienced in isolation, and we can describe the number of mutant phage V_{mut} as

$$V_{mut} = V_{mut}(t=0)e^{r_{res}(1+s_{comp})t}. \tag{8}$$

Given that in these simulations the two populations start with equal numbers, we can find the selective advantage in a competitive environment by tracking the relative number of mutant and resident

$$\frac{V_{mut}}{V_{res}} = \frac{V_{mut}(t=0)e^{r_{res}(1+s_{comp})t}}{V_{res}(t=0)e^{r_{res}t}} = e^{r_{res}s_{comp}t}. \tag{9}$$

As before, s_{comp} is determined from the average of many simulations. This approach allows us to measure the competitive selective advantage (s_{comp}) in both co-infecting (s_{co}) and non co-infecting (s_{nonco}) scenarios.

Measuring mutant probability of fixation

Once our simulations had been allowed to reach steady state, we introduced a single "mutant" phage into the free phage population, and the simulation was run until fixation or extinction occurs. This process was repeated at least 14 million times for each set of parameters. The probability of mutant fixation P_{fix} is determined from the fraction of simulations where the mutant fixed n_{fix} relative to the total number of simulations run n (i.e. $P_{fix} = n_{fix}/n$). Mutant fixation in this instance is a Poisson process, and so the error in mutant fixation probability ΔP_{fix} will be given by $\Delta P_{fix} = \sqrt{n_{fix}}/n$.

Results

Co-infection results in a larger effective population

We find that genetic diversity consistently declines faster in populations that prevent co-infection, indicating a smaller effective population size when compared to co-infecting populations. Fig. 2 shows that in both co-infecting and non co-infecting viral populations increasing adsorption rate and burst size, and decreasing lysis time result in larger effective populations. This observation is, however, partially attributable to the change in total phage population $N_T = (V_{ss} + \beta I_{ss})$, where V_{ss} indicates the steady state free phage population. I_{ss} indicates the steady state number of infected bacteria, and so βI_{ss} represents the number of phage that inevitably will join the free phage population shortly.

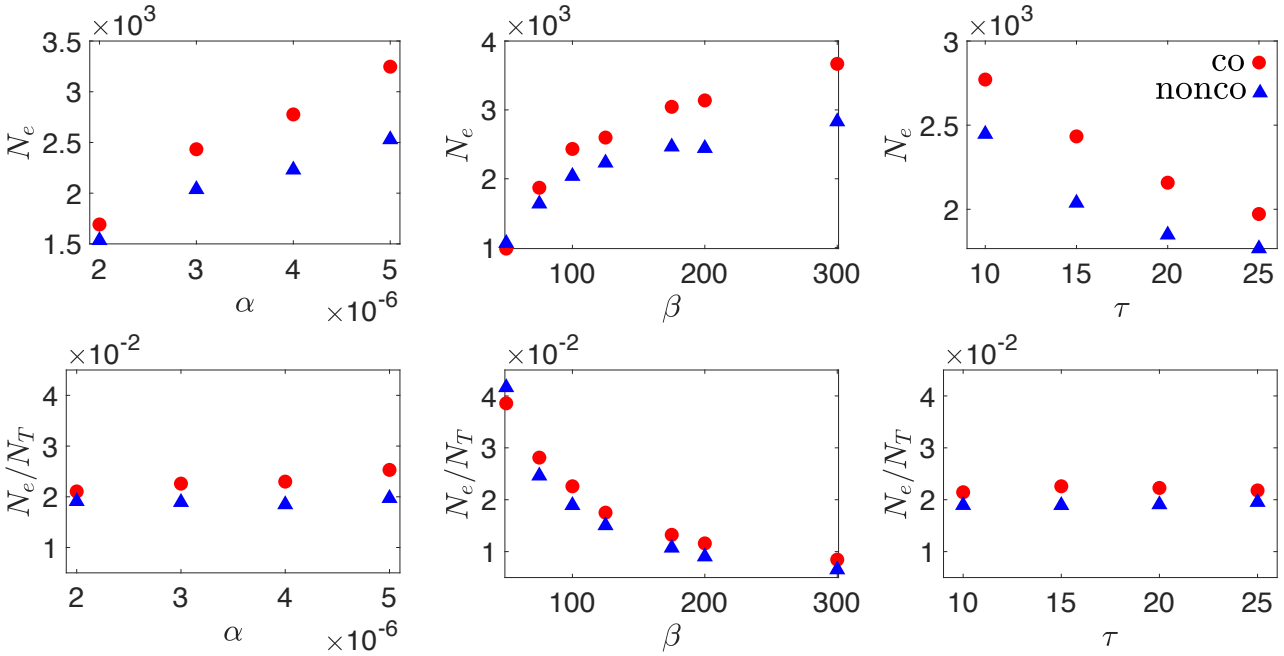

Figure 2. The effective population size in both co-infecting and non co-infecting populations as a function of adsorption rate α, burst size β and lysis time τ. Populations also shown scaled by the size of the total phage population $N_T = (V_{ss} + \beta I_{ss})$. Parameters used were $\alpha = 3 \times 10^{-6}$, $\beta = 100$ and $\tau = 15$ unless otherwise stated. As throughout, $\delta = 0.1$ and $B_0 = 1000$.

We find that while varying adsorption rate and lysis time impact both the effective and actual population sizes in the same way (i.e. $N_e/N_T \approx$ const.), as burst size is increased the effective population size reduces relative to the actual population size (Fig. 2). This can be intuitively explained by noticing that while increasing burst size results in more phage, and so larger effective and actual population sizes, the number of phage that can actually contribute to the next generation (i.e. the effective population size) is limited by the number of bacteria that are available. Therefore, as burst size is increased, an increasing fraction of phage in the population are unable to contribute and become wasted.

Neutral mutants fix slightly more often in co-infecting populations

To continue our characterisation of the neutral dynamics in both co-infecting and non co-infecting populations, we turn to the fixation probabilities of neutral mutants, and determine how they are affected by the phage infection parameters (adsorption rate α, burst size β and lysis time τ).

We vary one parameter at a time and measure the probability of fixation P_{fix}. To account for the different initial mutant frequency associated with different life history parameters, we rescale the fixation probability by the initial frequency of the mutant $f_0^* = 1/(V_{ss} + \beta I_{ss})$. Fig. 3 shows that $P_{fix}/f_0^* \approx 1$ as the parameters are varied, indicating that the total number of phages for a given set of parameters is the main controller of neutral dynamics. Indeed, we find that the impact of the life history parameters on the probability of fixation is what one would intuitively expect (Supporting Information, Fig. S4): increased adsorption rate and burst size, and reduced lysis time, all increase the steady-state size of the phage population, and reduce P_{fix}. This is supported by numerical solutions to a system of ordinary differential equations (ODEs) which describe the average behaviour of our model. The ODE solution shows that the total phage population at steady-state N_T is the same as in the stochastic model (Supporting Information, Fig. S4).

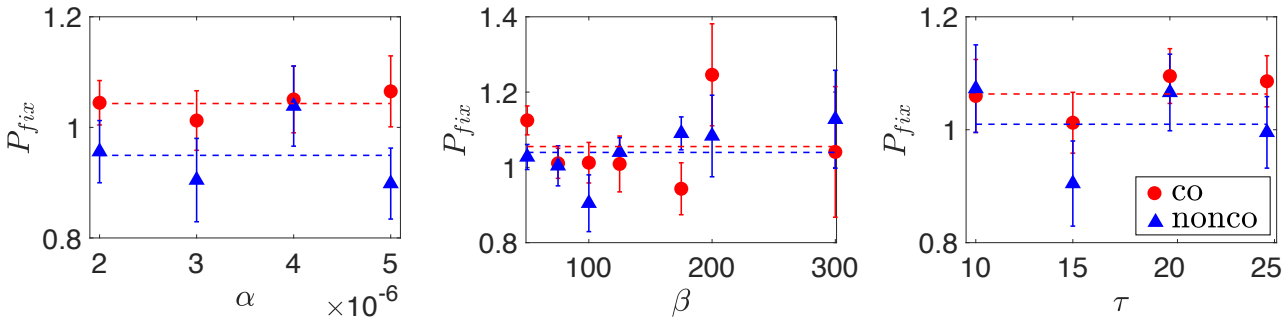

Figure 3. Probability of mutant fixation P_{fix} in the co-infecting and non co-infecting scenarios, scaled by the initial frequency of the mutant $f_0^* = 1/(V_{ss} + \beta I_{ss})$, as a function of adsorption rate α, burst size β and lysis time τ. Dashed lines indicate the simple average of the data for both the co-infecting (blue) and non co-infecting (red) scenarios. These lines indicate that neutral mutants in co-infecting populations experience a small advantage over mutants in an equivalent non co-infecting population. Unscaled P_{fix} data can be seen in Supporting Information, Fig. S4. Unless otherwise stated, the parameters used were $\alpha = 3 \times 10^{-6}$, $\beta = 100$, $\tau = 15$, $\delta = 0.1$ and $B_0 = 1000$.

Fig. 3 also shows that, on average, neutral mutants in the co-infecting scenario fix slightly more often than mutants in an equivalent non co-infecting population (blue and red dashed lines in Fig. 3 respectively). This result is similar to that found by Wodarz *et al.*, who showed that in a co-infecting viral population, higher multiplicities of infection offered a slight advantage to rare mutants that was not present at low multiplicities of infection[45]. This can be understood by noting that in the period shortly after the introduction of a mutant, in the co-infecting scenario, the mutant can increase in number by adsorbing to both uninfected and infected cells. By contrast, the resident phage can only increase in number by adsorbing to uninfected cells, because at this stage all infected cells are already infected with resident phage. As a result, the mutant has a slight advantage during the initial stages of growth which does not have in the non co-infecting scenario (or the low multiplicity of infection regime in Ref.[45], where co-infection is possible but rare).

Higher growth rate does not translate into competitive advantage

We now turn our attention to non-neutral mutations, and first characterise how phage growth rate and fitness is affected by changes to the phage infection parameters. As described in the Methods, we investigated the change in both growth rate and competitive fitness that are associated with changes in either the adsorption rate α, the burst size β or the lysis time τ, relative to the values used in our neutral simulations (Fig. 3).

Fig. S5 shows that either increasing burst size β or adsorption rate α result in a larger selective advantage s (both s_{growth} and s_{comp}), which is not surprising. We find that changes in burst size affect similarly the growth rate of the viral population in isolation and its (dis)advantage in a competitive setting (i.e. $s_{growth} \approx s_{comp}$, Fig. 4). Adsorption rate, however, leads to a stronger competitive (dis)advantage than what is determined by the growth rate in isolation (i.e. $s_{growth} < s_{comp}$). This likely originates from the fact that increasing adsorption rate is particularly advantageous in a competitive environment, as being the *first* virus to infect a host allows the virus to largely (co-infection) or completely (non co-infection) take the host for itself to reproduce.

The impact of altering lysis time τ is surprising. Fig. S5 shows that increasing τ results in a reduced growth rate (reduction in s_{growth}), as one might expect. On the other hand, Fig. 4 shows that varying τ has no discernible impact on s_{comp}. This

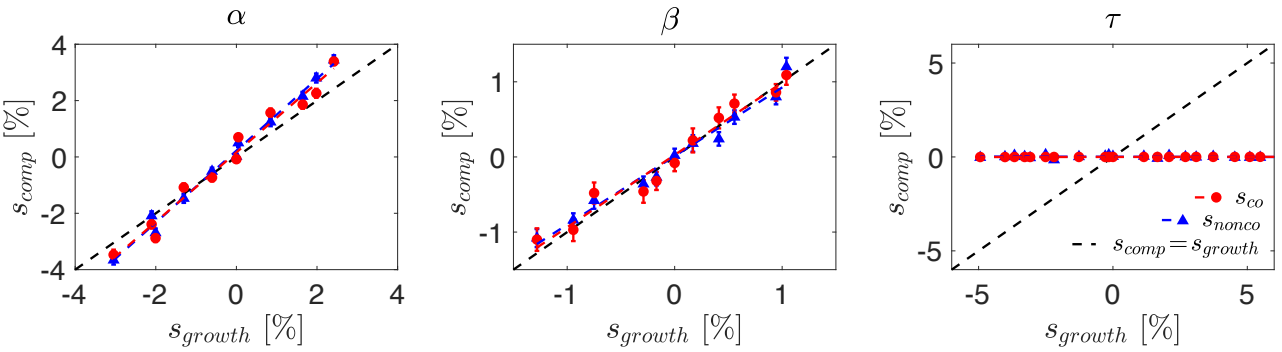

Figure 4. The selective advantage in a competitive setting s_{comp} as a function of the change in growth rate s_{growth}, when changing adsorption rate α, burst size β and lysis time τ. Resident parameters used were $\alpha = 3 \times 10^{-6}$, $\beta = 100$ and $\tau = 15$. As before $\delta = 0.1$ and $B_0 = 1000$. Error bars on x axis have been omitted for clarity.

observation is supported by our ODE model (Supporting Information), that shows that once the system is at steady-state, alterations to lysis time offer no advantage to one phage over the other (Fig. S6). This is likely an effect of the turbidostat setting we mimic in our model, which immediately replaces lysed hosts with uninfected cells. Therefore, no matter how long the phage take to lyse the cells, there are always the same number of viable hosts available for new phage to infect.

Co-infection results in more efficient selection

Having characterised how changes to the phage infection parameters alter first genetic drift and second fitness, we now put both aspects together and investigate the dynamics of non-neutral mutants. To this end,we simulate a resident phage population to steady state, then introduce a single non-neutral mutant and run the simulation until extinction or fixation occurs.

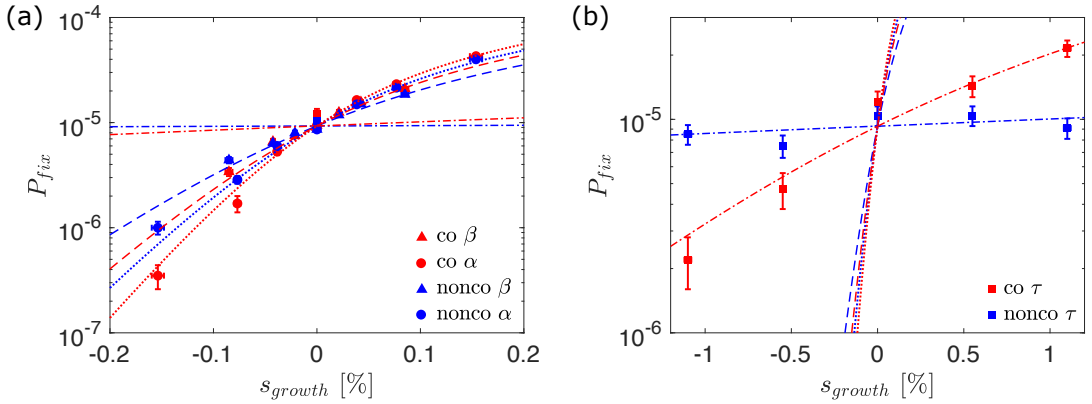

Figure 5. Effective population size and efficiency of selection. Probability of mutant fixation P_{fix} as a function of selective growth advantage s_{growth}. Points indicate simulation results, while lines, for (a) α and β indicate theoretically predicted values in a Moran model with equivalent parameters (Eq. 10). Lines for (b) τ show an optimised fit to the Moran model, with $s = \sigma s_{growth}$, as we were unable to measure the relationship between s_{growth} and s_{comp} (see Fig. 4). We find $\sigma_{nonco} = 0.008$ and $\sigma_{co} = 0.075$.

In agreement with our observations in Fig. 4 regarding the difference between growth rate and competitive fitness, we see in Fig. 5 that the same s_{growth} can lead to different fixation probabilities. We find again that a mutation that alters the adsorption rate α increases/decreases the mutant's chance to fix more than a mutation which alters the burst size β, even if both mutations have the same impact on growth rate. We can also see that beneficial mutations fix more often and deleterious mutations fix less often in co-infecting populations (red) than non co-infecting populations (blue). This suggests that selection is more efficient in co-infecting populations, as it fixes beneficial mutations and purges deleterious ones more readily.

To provide a theoretical framework to our findings, we compare the simulation data to the fixation probabilities one would

expect in a Moran model. For small selective advantage s, one expects that the probability of fixation will be equal to

$$P_{fix} = \frac{1 - e^{-N_e s f_0}}{1 - e^{-N_e s}}, \tag{10}$$

where f_0 is the initial frequency of the mutant in the population with effective population size N_e[50,52]. For α and β, we have independent measurements of the parameters in Eq. 10: $f_0 = f_0^*$ from our initial condition; N_e measured from the decay of heterozygosity (Fig. 2); and $s = s_{comp}(s_{growth})$ from our measurements of the relationship between competitive and growth rate advantage (Fig. 4). These theoretical predictions are plotted without additional fitting parameters as lines in Fig. 5. For τ mutants, we were unable to measure the relationship between s_{growth} and s_{comp} (Fig. 4), and so here we use a fitting parameter σ such that $s_{comp} = \sigma s_{growth}$. We find $\sigma_{nonco} = 0.008$ and $\sigma_{co} = 0.075$.

We can see in Fig. 5 that the theoretical prediction from the Moran model (Eq. 10) matches the simulation data very well. We note that in the co-infecting case, selection is *slightly* weaker than would be predicted by theory (Supporting Information), although still more efficient than the non co-infecting scenario. The difference likely arises from the effect outlined in Fig. 3, where rare mutants initially experience a slight advantage in the co-infecting scenario because they are able to increase in number by infecting both uninfected and infected cells, therefore making selection appear slightly weaker than would be expected by the Moran model where this effect is not present. To test the validity of our findings across parameter space, we also perform all of the above analysis with different resident parameters, with the same results (Supporting Information).

Preventing co-infection slows down adaptability in the long run, but is a winning strategy in the short term

Co-infection results in more efficient selection, meaning beneficial mutations are relatively more likely to fix, and deleterious ones are more likely to be purged, leading to a fitter overall population in the long run. From this point of view, allowing co-infection ultimately seems like the better long-term strategy when compared to preventing it. It is therefore puzzling why several natural phage populations have developed sophisticated mechanisms to prevent co-infection, particularly given that employing these mechanisms likely comes with a biological cost, such as reduced burst size[53,54] or increased lysis time[55], in addition to the loss of selection efficiency.

To address this question, we consider the fate of mutations that either (i) remove the mutant's ability to prevent co-infection in a resident non co-infecting population or (ii) provide the mutant the ability to prevent co-infection in a resident co-infecting population. Fig. 6 shows that if the mutant is neutral ($\beta_{mut} = \beta_{res} = 100$), then the non co-infecting mutant fixes two orders of magnitude more frequently than would otherwise be expected, based on its initial frequency f_0^*, and that the co-infecting mutant fixes at least more than two orders of magnitude less often (in our simulations this is the frequency we would be able to detect based on the number of iterations, but in reality we find no instances of mutant fixation). This indicates that mutants which are able to prevent co-infection experience a very strong selective advantage over their co-infecting counterparts, and vice-versa.

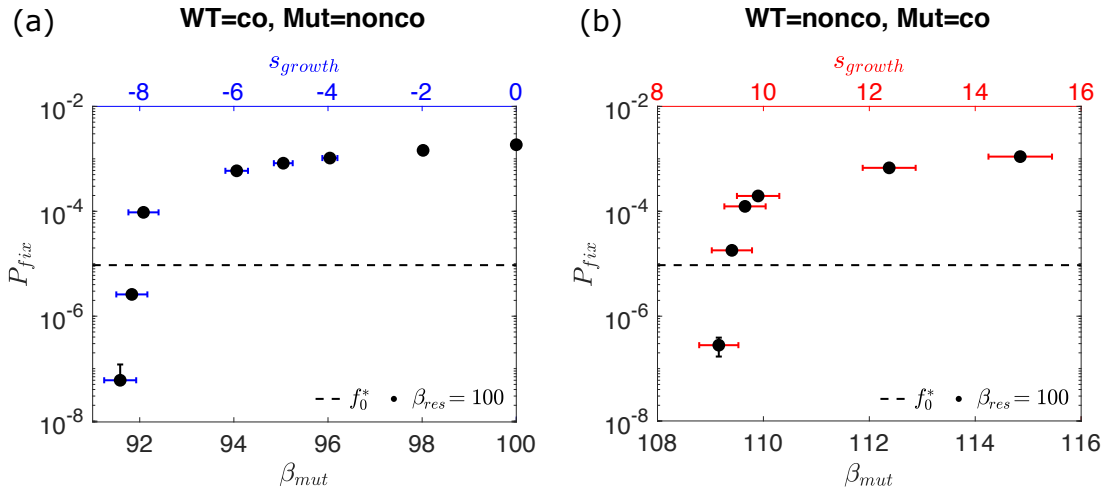

Figure 6. (a) The probability P_{fix} of a mutant which prevents co-infection fixing in a population that allows it, as a function of mutant burst size β_{mut}. (b) The probability P_{fix} of a mutant which allows co-infection fixing in a population that prevents it, as a function of mutant burst size β_{mut}. It can be seen that the co-infecting mutant requires a significantly increased burst size to fix, and conversely the non co-infecting mutant can fix, even if its burst size is greatly reduced.

The ability to prevent co-infection is likely to have some negative impact on the growth rate of the phage, as preventing co-infection will require the production of extra proteins, the resources for which could otherwise have gone to the production

of more phage. To determine what is the maximum burden that a non co-infecting mutant can sustain and still be able to fix, we consider the case where preventing co-infection results in a reduction in burst size[53]. Remarkably, we find that even when preventing co-infection comes at the cost of 8% reduction in burst size (≈8% change in s_{growth}), the non co-infecting mutant still fixes more often than a neutral co-infecting mutant (Fig. 6). Similarly, for a co-infecting mutant to have any chance of fixing in a non co-infecting population it requires at least a 9% increase in burst size (≈9% increase in s_{growth}). This indicates that while allowing co-infection increases selection efficiency at the population level, preventing it is ultimately a winning strategy in the short term, possibly explaining why phage capable of preventing co-infection are so common in nature[3,4].

Discussion

In this work, we have considered the impact of either allowing or preventing co-infection on the evolution of viral populations. Using a stochastic model of viral infection, we have shown that allowing co-infection reduces the strength of genetic drift, which can be viewed as an increase in effective population size. This increases the efficiency of selection in viral populations, with beneficial mutations fixing more frequently, and deleterious ones more readily being purged from the population. Despite the long term, population-wide benefit of allowing co-infection, once a mutant arises which is capable of preventing co-infection, that mutant will be strongly preferentially selected, even if its growth rate is greatly reduced. Once the whole population is capable of preventing co-infection, mutants which allow it similarly find it almost impossible to succeed.

The results we have presented here can be viewed in the context of the Prisoner's Dilemma, similar to the experimental work on RNA phage $\phi 6$ presented in[26,27]. In our work, phage can either allow or prevent co-infection, which in the context of the Prisoner's Dilemma can be seen as either 'co-operating' by sharing the host's resources or 'defecting' by acting selfishly and keeping all of the host's resources to oneself respectively. Overall the 'best' outcome occurs when all individuals co-operate, because allowing co-infection increases the efficiency of selection, making it easier to fix beneficial mutations and purge deleterious ones, in the long run increasing the fitness of the population. However, analogous to the Prisoner's Dilemma, in a population of co-operators a mutant phage can gain a significant reward by defecting (preventing co-infection), as it greatly increases it's chances of fixation. Conversely, in a population of defectors, a mutant co-operator is severely punished as it has a very low probability of fixation, and so in this situation it is also in the interest of the mutant to be a defector. Therefore, as in the Prisoner's Dilemma, while mutual co-operation yields overall the best outcome, defection is the *dominant strategy*, because it always results in a better outcome regardless of the other side's strategy.

Another interesting finding of our work is that in the turbidostat system we consider, while increased adsorption rate and burst size both increase the fitness of the phage population in all respects, lysis time does not play a role in the competitive dis(advantage) experienced once the system has reached a steady-state. It has been shown previously that in well-mixed liquid cultures where there is an abundant supply of hosts, generally higher adsorption rates and lower lysis times result in an increase in phage fitness[48,56,57]. The key difference there is that unlike the turbidostat system, host cells are not maintained at a constant density, and so there is no steady-state levels to be reached - the phage population will continue to grow until no bacteria remain. The differing impacts of the phage life-history parameters in well-mixed settings with and without a steady-state could have important implications for studies into the co-evolution of phage and bacteria populations using continuous culturing set-ups[58–60].

This difference also naturally begs the question of what influence lysis time, and the other parameters, would have in additional situations where steady-states are not reached, such as in continuous range expansions. The relationship between viral fitness and the phage life-history parameters (adsorption rate, lysis time and burst size) has been shown to be quite different, in both well-mixed[61] and spatially structured settings[62]. It has also been shown previously that eco-evolutionary feedbacks at the edge of expanding viral populations can result in travelling waves where the decline of genetic diversity is significantly reduced[63]. It would be interesting in future work to explore how allowing or preventing co-infection alters the eco-evolutionary dynamics of spatially expanding viral populations.

Acknowledgements

MH acknowledges studentship funding from EPSRC under grant number EP/R513180/1. This work was performed using resources provided by the Cambridge Service for Data Driven Discovery (CSD3) operated by the University of Cambridge Research Computing Service, provided by Dell EMC and Intel using Tier-2 funding from the Engineering and Physical Sciences Research Council (capital grant EP/P020259/1), and DiRAC funding from the Science and Technology Facilities Council.

Author Contributions

MH and DF conceived and designed the analysis; MH collected the data and performed the analysis; MH and DF wrote the paper.

References

1. Roux, S., Hallam, S. J., Woyke, T. & Sullivan, M. B. Viral dark matter and virus–host interactions resolved from publicly available microbial genomes. *eLife* **4**, DOI: 10.7554/eLife.08490.001 (2015).
2. Díaz-Muñoz, S. L. Viral coinfection is shaped by host ecology and virus-virus interactions across diverse microbial taxa and environments. *Virus Evol.* **3**, DOI: 10.1093/ve/vex011 (2017).
3. Labrie, S. J., Samson, J. E. & Moineau, S. Bacteriophage resistance mechanisms. *Nat. Rev. Microbiol.* **8**, 317–327, DOI: 10.1038/nrmicro2315 (2010).
4. van Houte, S., Buckling, A. & Westra, E. R. Evolutionary Ecology of Prokaryotic Immune Mechanisms. *Microbiol. molecular biology reviews : MMBR* **80**, 745–63, DOI: 10.1128/MMBR.00011-16 (2016).
5. Braun, V., Killmann, H. & Herrmann, C. Inactivation of FhuA at the cell surface of Escherichia coli K-12 by a phage T5 lipoprotein at the periplasmic face of the outer membrane. *J. Bacteriol.* **176**, 4710–4717, DOI: 10.1128/jb.176.15.4710-4717.1994 (1994).
6. Pedruzzi, I., Rosenbusch, J. P. & Locher, K. P. Inactivation in vitro of the Escherichia coli outer membrane protein FhuA by a phage T5-encoded lipoprotein. *FEMS Microbiol. Lett.* **168**, 119–125, DOI: 10.1111/j.1574-6968.1998.tb13264.x (1998).
7. Lu, M. J., Stierhof, Y. D. & Henning, U. Location and unusual membrane topology of the immunity protein of the Escherichia coli phage T4. *J. Virol.* **67** (1993).
8. Lu, M. J. & Henning, U. Superinfection exclusion by T-even-type coliphages. *Trends Microbiol.* **2**, 137–139, DOI: 10.1016/0966-842X(94)90601-7 (1994).
9. Frank, S. A. All of life is social, DOI: 10.1016/j.cub.2007.06.005 (2007).
10. Weitz, J. S., Mileyko, Y., Joh, R. I. & Voit, E. O. Collective decision making in bacterial viruses. *Biophys. J.* **95**, 2673–2680, DOI: 10.1529/biophysj.108.133694 (2008).
11. Refardt, D. Within-host competition determines reproductive success of temperate bacteriophages. *ISME J.* **5**, 1451–1460, DOI: 10.1038/ismej.2011.30 (2011).
12. Ojosnegros, S., Perales, C., Mas, A. & Domingo, E. Quasispecies as a matter of fact: Viruses and beyond, DOI: 10.1016/j.virusres.2011.09.018 (2011).
13. Koelle, K., Farrell, A. P., Brooke, C. B. & Ke, R. Within-host infectious disease models accommodating cellular coinfection, with an application to influenza†. *Virus Evol.* **5**, 18, DOI: 10.1093/ve/vez018 (2019).
14. Iranzo, J., Faure, G., Wolf, Y. I. & Koonin, E. V. Game-Theoretical Modeling of Interviral Conflicts Mediated by Mini-CRISPR Arrays. *Front. Microbiol.* **11**, 381, DOI: 10.3389/fmicb.2020.00381 (2020).
15. Vafadar, S., Shahdoust, M., Kalirad, A., Zakeri, P. & Sadeghi, M. Competitive exclusion during co-infection as a strategy to prevent the spread of a virus: A computational perspective. *PLOS ONE* **16**, e0247200, DOI: 10.1371/journal.pone.0247200 (2021).
16. Sanjuán, R. & Domingo-Calap, P. Genetic Diversity and Evolution of Viral Populations. In *Encyclopedia of Virology*, 53–61, DOI: 10.1016/b978-0-12-809633-8.20958-8 (Elsevier, 2021).
17. Bretscher, M. T., Althaus, C. L., Müller, V. & Bonhoeffer, S. Recombination in HIV and the evolution of drug resistance: for better or for worse? *BioEssays* **26**, 180–188, DOI: 10.1002/bies.10386 (2004).
18. Vijay, N. N., Vasantika, Ajmani, R., Perelson, A. S. & Dixit, N. M. Recombination increases human immunodeficiency virus fitness, but not necessarily diversity. *J. Gen. Virol.* **89**, 1467–1477, DOI: 10.1099/vir.0.83668-0 (2008).
19. Weller, S. K. & Sawitzke, J. A. Recombination Promoted by DNA Viruses: Phage λ to Herpes Simplex Virus. *Annu. Rev. Microbiol.* **68**, 237–258, DOI: 10.1146/annurev-micro-091313-103424 (2014).
20. Gao, H. & Feldman, M. W. Complementation and epistasis in viral coinfection dynamics. *Genetics* **182**, 251–263, DOI: 10.1534/genetics.108.099796 (2009).
21. Froissart, R. *et al.* Co-infection Weakens Selection Against Epistatic Mutations in RNA Viruses. *Genetics* **168**, 9–19, DOI: 10.1534/genetics.104.030205 (2004).
22. García-Arriaza, J., Manrubia, S. C., Toja, M., Domingo, E. & Escarmís, C. Evolutionary Transition toward Defective RNAs That Are Infectious by Complementation. *J. Virol.* **78**, 11678–11685, DOI: 10.1128/jvi.78.21.11678-11685.2004 (2004).

23. García-Arriaza, J., Ojosnegros, S., Dávila, M., Domingo, E. & Escarmís, C. Dynamics of Mutation and Recombination in a Replicating Population of Complementing, Defective Viral Genomes. *J. Mol. Biol.* **360**, 558–572, DOI: 10.1016/j.jmb.2006.05.027 (2006).

24. Gelderblom, H. C. *et al.* Viral complementation allows HIV-1 replication without integration. *Retrovirology* **5**, 60, DOI: 10.1186/1742-4690-5-60 (2008).

25. Turner, P. E. & Chao, L. Sex and the Evolution of Intrahost Competition in RNA Virus ϕ6. *Genetics* **150**, 523–532, DOI: 10.1093/genetics/150.2.523 (1998).

26. Turner, P. E. & Chao, L. Prisoner's dilemma in an RNA virus. *Nature* **398**, 441–443, DOI: 10.1038/18913 (1999).

27. Turner, P. E. & Chao, L. Escape from prisoner's dilemma in RNA phage ϕ6. *Am. Nat.* **161**, 497–505, DOI: 10.1086/367880 (2003).

28. Dennehy, J. J., Duffy, S., O'Keefe, K. J., Edwards, S. V. & Turner, P. E. Frequent Coinfection Reduces RNA Virus Population Genetic Diversity. *J. Hered.* **104**, 704–712, DOI: 10.1093/jhered/est038 (2013).

29. Donahue, D. A., Bastarache, S. M., Sloan, R. D. & Wainberg, M. A. Latent HIV-1 Can Be Reactivated by Cellular Superinfection in a Tat-Dependent Manner, Which Can Lead to the Emergence of Multidrug-Resistant Recombinant Viruses. *J. Virol.* **87**, 9620–9632, DOI: 10.1128/jvi.01165-13 (2013).

30. Chao, L. Evolution of sex in RNA viruses, DOI: 10.1016/0169-5347(92)90207-R (1992).

31. Asatryan, A., Wodarz, D. & Komarova, N. L. New virus dynamics in the presence of multiple infection. *J. Theor. Biol.* **377**, 98–109, DOI: 10.1016/j.jtbi.2015.04.014 (2015).

32. Dixit, N. M. & Perelson, A. S. Multiplicity of Human Immunodeficiency Virus Infections in Lymphoid Tissue. *J. Virol.* **78**, 8942–8945, DOI: 10.1128/jvi.78.16.8942-8945.2004 (2004).

33. Dixit, N. M. & Perelson, A. S. HIV dynamics with multiple infections of target cells. *Proc. Natl. Acad. Sci. United States Am.* **102**, 8198–8203, DOI: 10.1073/pnas.0407498102 (2005).

34. Althaus, C. L. & Bonhoeffer, S. Stochastic Interplay between Mutation and Recombination during the Acquisition of Drug Resistance Mutations in Human Immunodeficiency Virus Type 1. *J. Virol.* **79**, 13572–13578, DOI: 10.1128/jvi.79.21.13572-13578.2005 (2005).

35. Fraser, C. HIV recombination: What is the impact on antiretroviral therapy? *J. Royal Soc. Interface* **2**, 489–503, DOI: 10.1098/rsif.2005.0064 (2005).

36. Wodarz, D. & Levy, D. N. Effect of different modes of viral spread on the dynamics of multiply infected cells in human immunodeficiency virus infection. *J. Royal Soc. Interface* **8**, 289–300, DOI: 10.1098/rsif.2010.0266 (2011).

37. Cummings, K. W., Levy, D. N. & Wodarz, D. Increased burst size in multiply infected cells can alter basic virus dynamics. *Biol. Direct* **7**, 16, DOI: 10.1186/1745-6150-7-16 (2012).

38. May, R. M. & Nowak, M. A. Superinfection, metapopulation dynamics, and the evolution of diversity. *J. Theor. Biol.* **170**, 95–114, DOI: 10.1006/jtbi.1994.1171 (1994).

39. Nowak, M. A. & May, R. M. Superinfection and the evolution of parasite virulence. *Proc. Royal Soc. B: Biol. Sci.* **255**, 81–89, DOI: 10.1098/rspb.1994.0012 (1994).

40. Van Baalen, M. & Sabelis, M. W. The dynamics of multiple infection and the evolution of virulence. *Am. Nat.* **146**, 881–910, DOI: 10.1086/285830 (1995).

41. Alizon, S. & Van Baalen, M. Multiple infections, immune dynamics, and the evolution of virulence. *Am. Nat.* **172**, 150–168, DOI: 10.1086/590958 (2008).

42. Alizon, S., de Roode, J. C. & Michalakis, Y. Multiple infections and the evolution of virulence. *Ecol. Lett.* **16**, 556–567, DOI: 10.1111/ele.12076 (2013).

43. Leeks, A., Segredo-Otero, E. A., Sanjuán, R. & West, S. A. Beneficial coinfection can promote within-host viral diversity. *Virus Evol.* **4**, DOI: 10.1093/ve/vey028 (2018).

44. Phan, D. & Wodarz, D. Modeling multiple infection of cells by viruses: Challenges and insights. *Math. Biosci.* **264**, 21–28, DOI: https://doi.org/10.1016/j.mbs.2015.03.001 (2015).

45. Wodarz, D., Levy, D. N. & Komarova, N. L. Multiple infection of cells changes the dynamics of basic viral evolutionary processes. *Evol. Lett.* **3**, 104–115, DOI: 10.1002/evl3.95 (2019).

46. Bryson, V. & Szybalski, W. Microbial selection, DOI: 10.1126/science.116.3003.45 (1952).

47. Gresham, D. & Dunham, M. J. The enduring utility of continuous culturing in experimental evolution. *Genomics* **104**, 399–405, DOI: 10.1016/j.ygeno.2014.09.015 (2014).

48. Wang, I.-N. Lysis Timing and Bacteriophage Fitness. *Genetics* **172**, 17–26 (2006).

49. Hallatschek, O. & Nelson, D. R. Gene surfing in expanding populations. *Theor. Popul. Biol.* **73**, 158–170, DOI: 10.1016/J.TPB.2007.08.008 (2008).

50. Moran, P. A. Random processes in genetics. *Math. Proc. Camb. Philos. Soc.* **54**, 60–71, DOI: 10.1017/S0305004100033193 (1958).

51. Fisher, R. A. & Bennett, J. H. *The Genetical Theory of Natural Selection: A Complete Variorum Edition* (OUP Oxford, 1999).

52. Dinh, K. N., Corey, S. J. & Kimmel, M. Application of the Moran Model in Estimating Selection Coefficient of Mutated CSF3R Clones in the Evolution of Severe Congenital Neutropenia to Myeloid Neoplasia. *Front. Physiol.* **11**, 806, DOI: 10.3389/fphys.2020.00806 (2020).

53. Delbrück, M. Interference between bacterial viruses; the mutual exclusion effect and the depressor effect. *J. bacteriology* **50**, 151–170 (1945).

54. Karam, J. D., Drake, J. W., Kreuzer, K. N., Hall, D. H. & Mosig, G. *Molecular Biology of Bacteriophage T4* (American Society for Microbiology, 1994).

55. Abedon, S. T. Lysis of lysis-inhibited bacteriophage T4-infected cells. *J. Bacteriol.* **174**, 8073–8080, DOI: 10.1128/jb.174.24.8073-8080.1992 (1992).

56. Wang, I. N., Dykhuizen, D. E. & Slobodkin, L. B. The evolution of phage lysis timing. *Evol. Ecol.* **10**, 545–558, DOI: 10.1007/BF01237884 (1996).

57. Shao, Y. & Wang, I. N. Bacteriophage adsorption rate and optimal lysis time. *Genetics* **180**, 471–482, DOI: 10.1534/genetics.108.090100 (2008).

58. Spanakis, E. & Horne, M. T. Co-adaptation of Escherichia coli and coliphage γvir in continuous culture. *J. Gen. Microbiol.* **133**, 353–360, DOI: 10.1099/00221287-133-2-353 (1987).

59. Mizoguchi, K. *et al.* Coevolution of bacteriophage PP01 and Escherichia coli O157:H7 in continuous culture. *Appl. Environ. Microbiol.* **69**, 170–176, DOI: 10.1128/AEM.69.1.170-176.2003 (2003).

60. Koskella, B. & Brockhurst, M. A. Bacteria-phage coevolution as a driver of ecological and evolutionary processes in microbial communities. *FEMS Microbiol. Rev.* **38**, 916–931, DOI: 10.1111/1574-6976.12072 (2014).

61. Bull, J. J., Heineman, R. H. & Wilke, C. O. The phenotype-fitness map in experimental evolution of phages. *PLoS ONE* **6**, 27796, DOI: 10.1371/journal.pone.0027796 (2011).

62. Kerr, B., Neuhauser, C., Bohannan, B. J. M. & Dean, A. M. Local migration promotes competitive restraint in a host-pathogen 'tragedy of the commons'. *Nature* **442**, 75–78, DOI: 10.1038/nature04864 (2006).

63. Hunter, M., Krishnan, N., Liu, T., Möbius, W. & Fusco, D. Virus-Host Interactions Shape Viral Dispersal Giving Rise to Distinct Classes of Traveling Waves in Spatial Expansions. *Phys. Rev. X* **11**, 21066, DOI: 10.1103/PhysRevX.11.021066 (2021).

Supporting Information

This Supporting Information (SI) contains expanded data analysis and derivations of the results presented in the main text. It also outlines an ordinary differential equation (ODE) model which describes the average behaviour of our system.

Contents

1 Steady-States Are Independent of Initial Conditions

This section serves to verify that our choice of initial condition ($V_0 = 2B_0$) does not impact the steady-state phage population V_{ss} reached in the stochastic simulations. Fig. S1 shows that V_{ss} remains constant across a wide range of V_0 values, thereby confirming the choice of V_0 is not important.

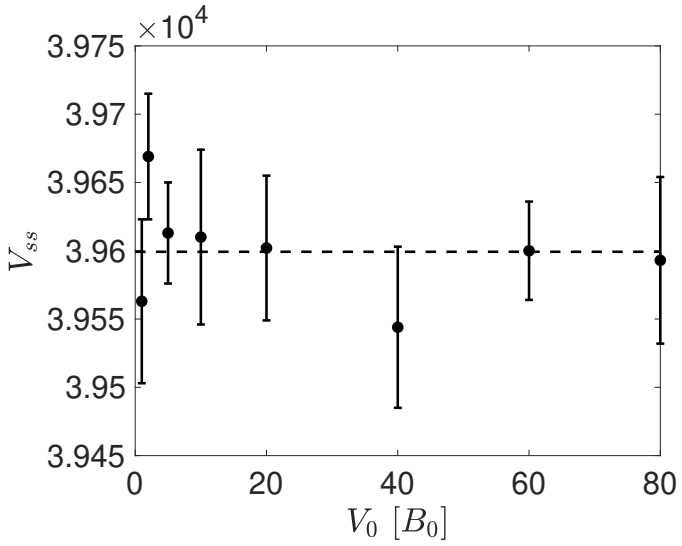

Figure S1. The steady-state phage population V_{ss} reached does not depend on the initial number of phage V_0 in the simulations. In all, $\alpha = 3 \times 10^{-6}$, $\beta = 100$, $\tau = 15$, $\delta = 0.1$ and $B_0 = 1000$.

2 Effective Population Size

Here we show an example of the average decay in heterozygosity $H = 2f(1-f)$, as a function of time, with f and $(1-f)$ representing the frequencies of two neutral labels in the population. We find (Fig. S2) that the heterozygosity decays due to genetic drift, and consistent with previous work [1], we find that the decay is exponential at long times: $H \propto e^{-\Lambda t}$. We can then express the decay rate, in units of generations (see Methods), in terms of an effective population size $\Lambda \equiv 2/N_e$ (Moran model [2]).

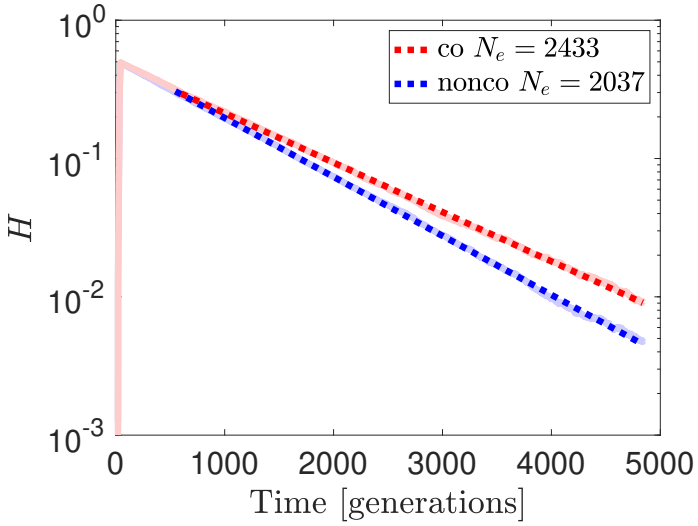

Figure S2. Linear fit to log transformed heterozygosity data, with slope $\Lambda \equiv 2/N_e$ revealing that allowing co-infection (red) results in a larger effective population size compared to the case where co-infection is prevented (blue). Parameters used were $\alpha = 3 \times 10^{-6}$, $\beta = 100$, $\tau = 15$, $\delta = 0.1$ and $B_0 = 1000$.

3 ODE Description of Model

The average behaviour of the model used in the main text can be described by a set of ordinary differential equations (ODEs):

$$\frac{dV}{dt} = -\alpha V(B+I) - \delta V + \beta\alpha V_{t-\tau}B_{t-\tau}, \tag{1a}$$

$$\frac{dB}{dt} = -\alpha VB + \alpha V_{t-\tau}B_{t-\tau}, \tag{1b}$$

$$\frac{dI}{dt} = \alpha VB - \alpha V_{t-\tau}B_{t-\tau}, \tag{1c}$$

where all of the symbols are defined the same as in the main text (V, B and I indicate the concentrations of phage, uninfected bacteria and infected bacteria as a function of time respectively; α, β, τ and δ indicate the phage adsorption rate, burst size, lysis time and decay rate respectively). The subscript is used to indicate that those terms are calculated at time $t - \tau$.

By numerically solving this ODE system, we can verify that for certain parameters, a steady state solution is reached where $V = V_{ss}$, $B = B_{ss}$ and $I = I_{ss}$, in agreement with the average behaviour of the stochastic model used throughout the main text (Fig. S3 and Fig. S4).

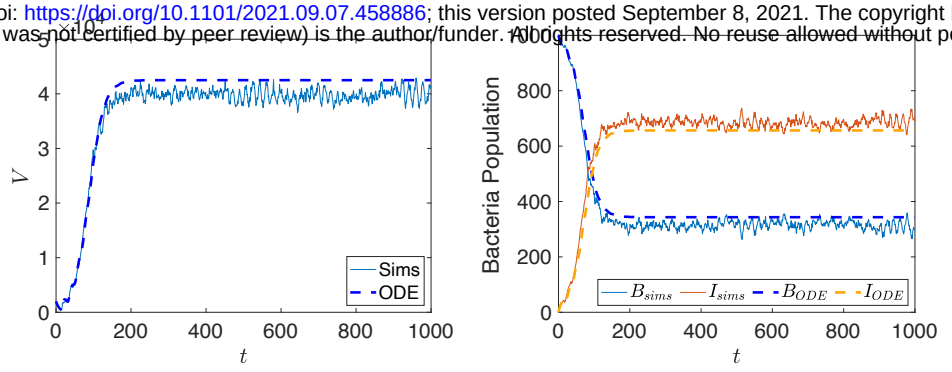

Figure S3. The average behaviour of the model in the main text is mostly captured by the ODE description set out in Eqs. 1. Slight discrepancies arise due to the fact that in the simulations, infection, decay and lysis must occur in discrete steps. Parameters used are $\alpha = 3 \times 10^{-6}$, $\beta = 100$, $\tau = 15$, $\delta = 0.1$ and $B_0 = 1000$.

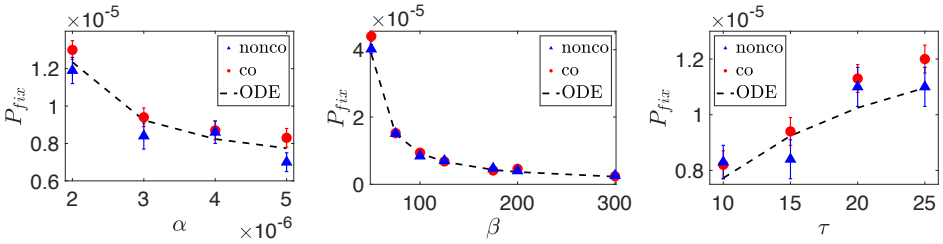

Figure S4. Probability of mutant fixation P_{fix} in the co-infecting and non co-infecting scenarios as a function of adsorption rate α, burst size β and lysis time τ. This is the same as the data displayed in Fig. 3 of the main text, prior to scaling by the initial frequency $f_0^* = 1/(V_{ss} + \beta I_{ss})$. Error bars are plotted, although in some instances may be too small to see. This data is compared with the solution of the system of ODEs, with the black dashed line represents the frequency f_0^* calculated from the steady-states reached.

4 Fitness Measurements

In Fig. S5 we present the fitness measurements made using our stochastic model, as the phage infection parameters (adsorption rate α, burst size β and lysis time τ) are varied. As described in the main text, fitness is measured both in terms of its effect on the growth rate in isolation (s_{growth}), and in terms of its effect in a competitive setting, by the relative change in frequency of two variants in a population (s_{nonco} and s_{co}).

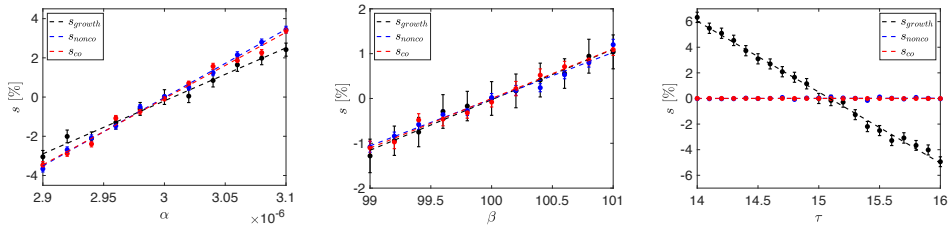

Figure S5. The selective advantage s relative to a resident phage that results from a change to adsorption rate α, burst size β and lysis time τ. This is measured both in terms of the effect on the isolated growth rate of the mutant (s_{growth}, Eq. 7), and in terms of the change in frequency in a population initiated with 50% mutant and 50% resident (s_{nonco} and s_{co}, Eq. 9). Resident parameters used were $\alpha = 3 \times 10^{-6}$, $\beta = 100$ and $\tau = 15$. As before $\delta = 0.1$ and $B_0 = 1000$.

In Fig. S6 we show using the ODE model, which describes the average behaviour of the system, that once the system has reached steady-state, altering lysis time has no impact on the relative frequency of two variants within the population (i.e. both variants appear neutral relative to one another). This

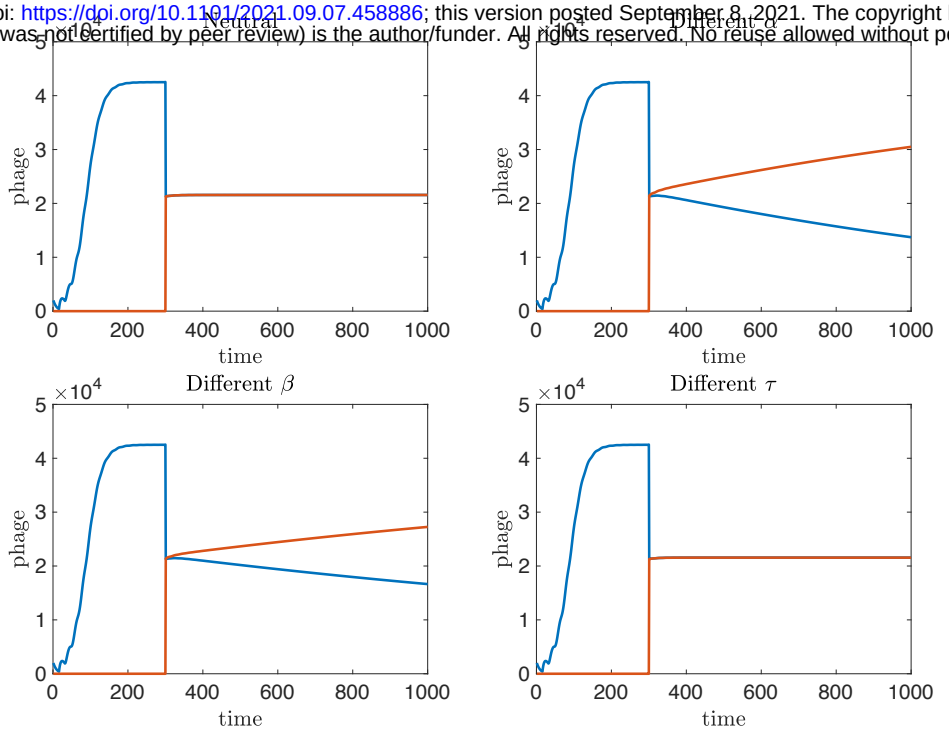

Figure S6. The relative change in frequency of two populations in the ODE model (indicating the average behaviour in the stochastic model). It can be seen that once at steady-state, changing lysis time τ has no effect. Parameters used were $\alpha = 3 \times 10^{-6}$, $\beta = 100$ and $\tau = 15$ unless otherwise stated. As throughout, $\delta = 0.1$ and $B_0 = 1000$.

supports the observation in the stochastic model that $s_{comp}(\tau) \approx 0$.

5 Comparison To Moran Model

If we introduce a free scaling parameter ϕ, such that $s = \phi s_{comp}$, and optimally fit Eq. 10 to the data, we can use the resulting value for ϕ as a quantitative measure of the quality of agreement between simulations and theory. It should be noted that while we have described the scaling in terms of s, it is mathematically identical to scaling N_e. Through this optimal fitting we find that $\phi_{n\alpha} = 1.050$, $\phi_{n\beta} = 1.028$, $\phi_{c\alpha} = 0.992$ and $\phi_{c\beta} = 0.986$, with subscripts indicating scenario and parameter combinations. This indicates that both scenarios agree with the Moran model to within 5%.

6 $\beta_{res} = 70$ Measurements

Here we repeat a subset of the measurements carried out in the main text for different resident phage parameters, in this instance $\beta_{res} = 70$, with all other parameters remaining the same as in the main text. First, the effective population size is measured in both co-infecting and non co-infecting populations (Fig. S7), demonstrating that N_e is larger in co-infecting populations.

We then move on to characterise the fitness of non-neutral mutants, in this instance only varying burst size β (Fig. S8). Again, we find a positive linear relationship between burst size and fitness, both in terms of the effect on growth rate in isolation and in a competitive setting. Interestingly here we find that alterations to burst size make slightly less difference in a competitive setting, as compared to the effect on growth rate. This could potentially be because, at lower burst sizes, any small change in β has a large impact on the growth rate, but has a smaller impact in a population already at steady state.

Finally, we put both aspects together and measure the probability of fixation of non-neutral mutants in both co-infecting and non co-infecting populations (Fig. S9). As in the main text, we find fairly good, although slightly worse, agreement between our simulation results and the prediction from a Moran model with our independently measured parameters (Fig. S7 and Fig. S8). In terms of the additional fitting parameter introduced in the previous section, we find here that $\phi_{co} = 0.83$ and $\phi_{nonco} = 0.90$. It's

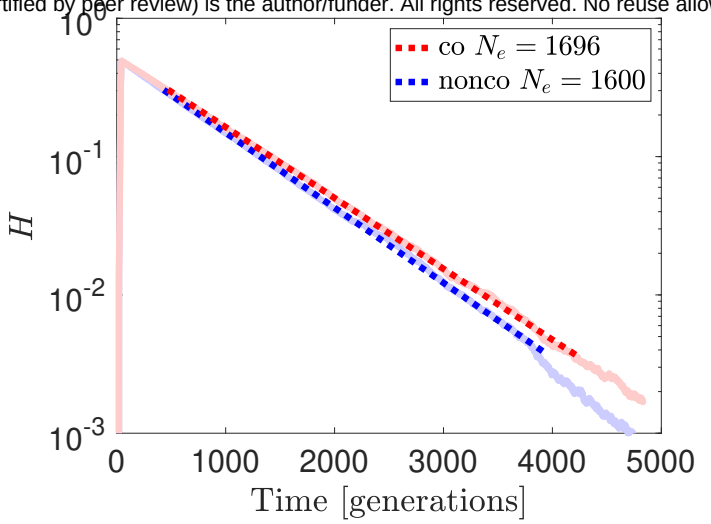

Figure S7. Linear fit to log transformed heterozygosity data, with slope $\Lambda \equiv 2/N_e$ revealing that allowing co-infection (red) results in a larger effective population size compared to the case where co-infection is prevented (blue). Parameters used were $\alpha = 3 \times 10^{-6}$, $\beta = 70$, $\tau = 15$, $\delta = 0.1$ and $B_0 = 1000$.

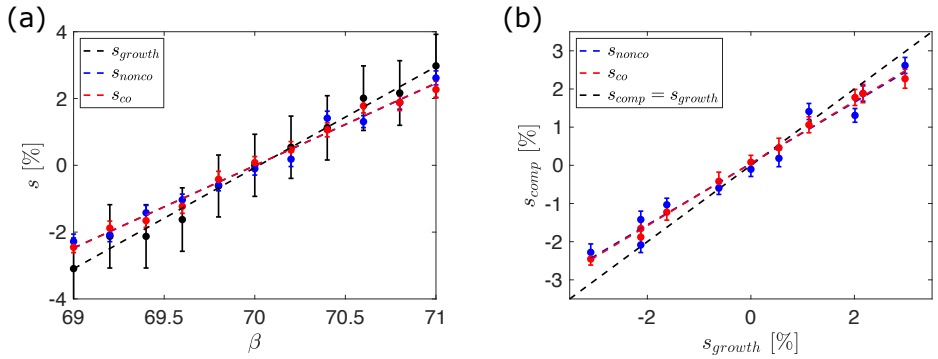

Figure S8. (a): The selective advantage s relative to a resident phage that results from a change to burst size β. This is measured both in terms of the effect on the isolated growth rate of the mutant (s_{growth}, Eq. 7), and in terms of the change in frequency in a population initiated with 50% mutant and 50% resident (s_{nonco} and s_{co}, Eq. 9). (b): The fitness in a competitive setting s_{comp} is then shown as a function of the fitness in an isolated setting s_{growth}. Resident parameters used were $\alpha = 3 \times 10^{-6}$, $\beta = 70$ and $\tau = 15$. As before $\delta = 0.1$ and $B_0 = 1000$.

possible that this discrepancy is caused by imprecision in the measurements of fitness as a function of burst size. Indeed, over the whole range of β we would not expect a perfect linear relationship between burst size and fitness, with the benefits of increased burst size being larger for small β, and so at these lower values of β we find that the linear fit is less of a good approximation.

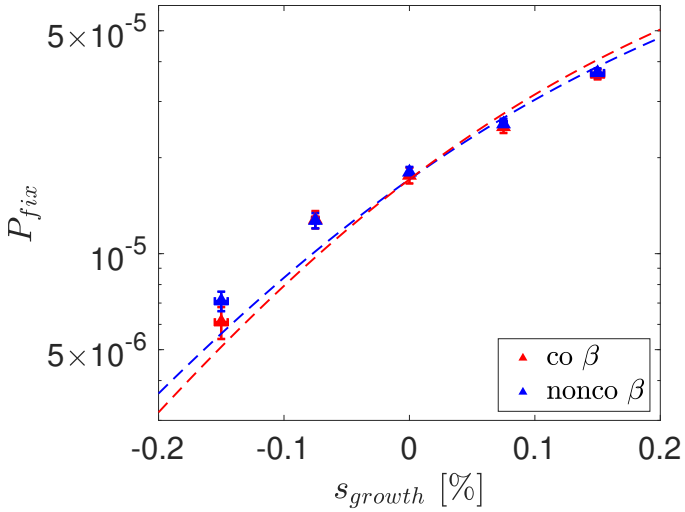

Figure S9. Probability of mutant fixation P_{fix} as a function of selective growth advantage s_{growth}. Points indicate simulation results, while lines indicate theoretically predicted values in a Moran model with equivalent parameters (Eq. 10).

References

[1] Oskar Hallatschek and David R. Nelson. Gene surfing in expanding populations. *Theoretical Population Biology*, 73(1):158–170, 2 2008.

[2] P. A.P. Moran. Random processes in genetics. *Mathematical Proceedings of the Cambridge Philosophical Society*, 54(1):60–71, 1958.